Thin Solid Films 519 (2011) 2488–2492

Contents lists available at ScienceDirect

Thin Solid Films

journal homepage: www.elsevier.com/locate/tsf

Aqueous bath process for deposition of Cu_2ZnSnS_4 photovoltaic absorbers

A. Wangperawong [a], J.S. King [b], S.M. Herron [c], B.P. Tran [b], K. Pangan-Okimoto [b], S.F. Bent [b,*]

[a] Department of Electrical Engineering, Stanford University, Stanford, CA 94305 USA
[b] Department of Chemical Engineering, Stanford University, Stanford, CA 94305 USA
[c] Department of Chemistry, Stanford University, Stanford, CA 94305 USA

ARTICLE INFO

Article history:
Received 4 August 2010
Received in revised form 24 November 2010
Accepted 24 November 2010
Available online 4 December 2010

Keywords:
Cu2ZnSnS4
Solution processing
Chemical bath deposition
Solar cell
Photovoltaics
CZTS
Chalcogenide

ABSTRACT

Chemical bath deposition and ion exchange were used to incorporate copper, zinc, tin and sulfur into a thin film precursor stack. The stack was then sulfurized to form the photovoltaic absorber material Cu_2ZnSnS_4 (CZTS). The morphology and elemental composition of the films at each process stage were analyzed by Auger electron spectroscopy and scanning electron microscopy, and the structural and optical properties of the sulfurized film were determined by a combination of X-ray diffraction, Raman scattering, and diffuse reflectance UV–Vis spectroscopy. Compositionally uniform microcrystalline CZTS with kesterite structure and a bandgap of 1.45 eV were observed. A preliminary solar cell device was produced exhibiting photovoltaic and rectifying behavior.

1. Introduction

Current leading thin-film solar cell materials, such as CdTe and CIGS, face the risk of production limitations at a global scale due to the scarce and toxic elements involved [1]. A material gaining significant attention in addressing these issues is Cu_2ZnSnS_4 (CZTS), which has an ideal single junction bandgap of 1.4–1.5 eV [2].

Several groups have investigated the fabrication of CZTS solar cells using a variety of methods including spray pyrolysis, evaporation, sputtering, sol-gel processing, electrodeposition, and nanocrystal synthesis [3–11]. Todorov et al. achieved a 9.7% efficient $Cu_2ZnSn(Se,S)_4$ device fabricated through a hydrazine-slurry method in an inert atmosphere, demonstrating the potential of CZTS and similar kesterite materials to be effective photovoltaic absorber layers [12].

Thus far, the absorber layers of the highest performing kesterite-based devices were deposited by evaporation, sputtering or hydrazine slurry-based methods. A potential drawback of these methods is the use of expensive and complicated machinery for mass production. Whereas the physical deposition methods require vacuum chambers and high power supplies, the hydrazine-based method requires equipment specifically designed for hydrazine, which is toxic and flammable. For the other solution and particle based methods that have been investigated, performance is typically limited by the final film quality after annealing or drying. Volume contraction upon drying induces residual stress, voids and cracks. Therefore methods that address both equipment complexity and film integrity should be considered.

Here we report an alternative method for deposition of CZTS thin films that has the potential to be scaled up to large area deposition for use in mass manufacturing of monolithically integrated solar panel modules with high throughput and low cost. Our aqueous approach is based on chemical bath deposition (CBD) [13] and ion exchange [14] of chalcogenide thin films, along with a subsequent sulfurization heat treatment. High materials utilization has previously been demonstrated through CBD [15].

Using scanning electron microscopy (SEM), Auger electron spectroscopy (AES), X-ray diffraction (XRD), Raman spectroscopy, inductively-coupled plasma optical emission spectroscopy (ICP-OES), and diffuse reflectance UV–Vis spectroscopy, we demonstrate that this inexpensive and relatively benign process produces thin films of CZTS exhibiting uniform composition, kesterite crystal structure, and good optical properties. A preliminary solar cell device was produced to demonstrate rectifying and photovoltaic behavior.

2. Experimental details

The substrates used – silicon, glass and Mo-coated silicon – were first cleaned using acetone, ethanol and deionized water and then mounted in the CBD bath according to Fig. 1.

SnS_x was grown at room temperature after the method of Nair et al. [16]. The deposition bath consisted of aqueous triethanolamine (12 mL, 3.7 M), tin chloride dihydrate dissolved in acetone (5 mL,

* Corresponding author. 381 North South Axis, Stanford University, Stanford, California 94305, USA. Tel.: +1 650 723 0385; fax: +1 650 723 9780.
E-mail address: sbent@stanford.edu (S.F. Bent).

0040-6090/$ – see front matter © 2010 Elsevier B.V. All rights reserved.
doi:10.1016/j.tsf.2010.11.040

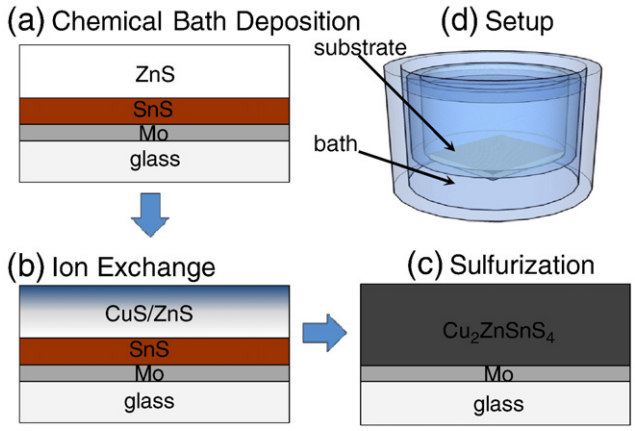

Fig. 1. (a)–(c) Chemical bath process steps and (d) experimental setup for depositing CZTS.

0.83 M), aqueous thioacetamide solution (5 mL, 0.91 M), deionized water (65 mL), and aqueous ammonia (10 mL, 4 M). After 18 h, the substrates were removed and rinsed with deionized water.

According to the method of Cheng et al. [17], a ZnS bath was next prepared with sodium citrate dihydrate (0.13 M), zinc acetate dihydrate (0.2 M), ammonium hydroxide (0.72 M), and thiourea (0.6 M). The bath was maintained for 1 h at 70 °C using a jacketed beaker or silicone oil bath. This process was performed twice to account for material loss during Cu ion exchange. The resulting SnS_x/ZnS precursor films were then annealed in air at 400 °C for 3 h. Cu was next incorporated into the bath-deposited films via ion exchange [18–20]. To carry out ion exchange, the SnS_x/ZnS-coated substrates were placed in an aqueous Cu^{2+} (0.1 M) bath for times ranging from 1 min to 4 h.

The precursor stacks were subsequently sulfurized for 2 h at 500 °C to form CZTS. A gas delivery system generated H_2S *in situ* through the decomposition of thioacetamide [21] and delivered it to the sample at a minimum pressure of 46.7 Pa. Thus, only the minimum amount of H_2S necessary is generated on demand.

A complete device was produced with the standard CIGS device architecture. The additional steps include 5 min of KCN treatment [22], 50 nm of CBD-deposited CdS [23], 100 nm of sputtered ZnO and 350 nm of Al:ZnO. For the top contact grid, silver paste was passed through a screen printer and heated at 200 °C for 30 min.

Scanning electron micrographs were obtained using an FEI XL30 Sirion SEM instrument at a 5.0 kV accelerating voltage. Auger electron spectra were collected using a PHI 700 Scanning Auger Nanoprobe instrument with Ar^+ sputtering to capture depth profiles. For ICP-OES, a TJA IRIS Advantage/1000 Radial ICAP Spectrometer was used to characterize ion-exchanged films dissolved in aqua regia and deionized water. X-ray diffraction spectra were acquired using a PANalytical X'Pert PRO diffractometer. Cu Kα radiation was used with 45 kV tension and 40 mA current, scanning the 2θ range of 20° to 50°. Raman measurements were performed with a Horiba LabRAM ARAMIS Confocal Raman Microscope equipped with a 532 nm laser. Diffuse reflectance spectra were acquired with an Ocean Optics ISP-50-8-R integrating sphere, an International Light RPS900 spectroradiometer and a Newport 1000 W Xe arc lamp.

3. Results and discussion

The morphology of the samples was analyzed using SEM. Fig. 2a shows a cross-sectional image after the first step of the process, the SnS_x deposition. The film appears uniform and adherent on top of the Mo layer. The lumpy morphology may be indicative of a cluster-by-cluster mechanism, where colloids that nucleate in the solution adsorb to the substrate, and then an ion-by-ion growth mechanism leads to coagulation [24].

Fig. 2b shows the resulting cross section after deposition of a single layer of ZnS and subsequent 400 °C heat treatment. There is minimal mixing of the ZnS and SnS_x layers, which is consistent with experimentally determined phase diagrams [25]. Fig. 2c shows the SnS_x/ZnS stack after 15 min of Cu^{2+} (0.1 M) exchange. The slight decrease in thickness is due to some dissolution of the film in the exchange solution. Subsequent precursor stacks utilized two layers of ZnS to address the issue of material loss. In general, the Zn and Sn amounts can be controlled by the film thicknesses, which are related to the deposition time.

Fig. 2d shows an SEM cross-section at 45º viewing angle of Cu–Zn–Sn precursor film on Si after a 2-hour heat treatment with H_2S. The nominal thickness of the resulting film is about 700 nm, suggesting that the process described here should be repeated several times to produce sufficiently thick photovoltaic absorber material. There is also some

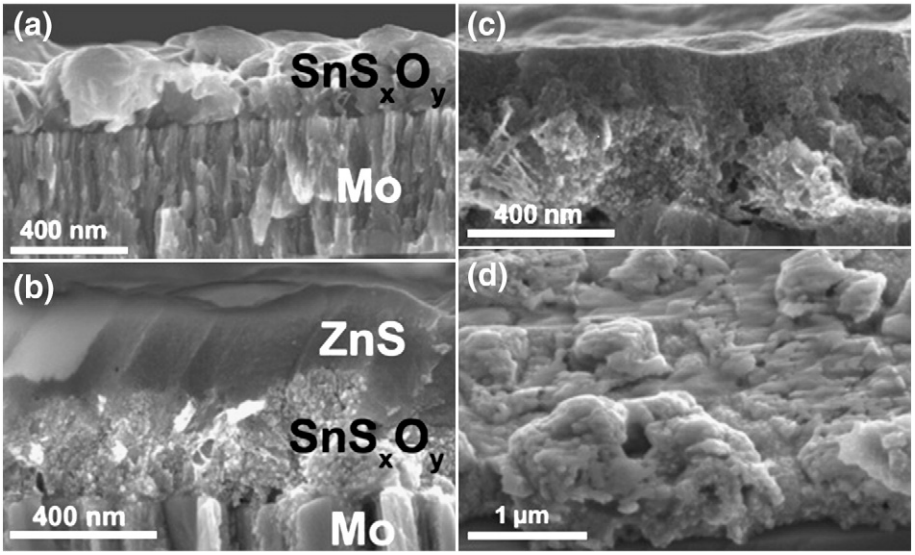

Fig. 2. SEM cross sections of (a) SnS_xO_y on Mo, (b) after ZnS deposition and 400 °C heat treatment, (c) after 15 min of Cu^{2+} (0.1 M) exchange, and (d) 45º view of 2-hour sulfurized Cu–Sn–Zn precursor film on Si.

surface texturing, which could be beneficial for light trapping as long as it does not cause shunting. From our studies, which are currently in progress, we have found that the surface texture depends on deposition temperature and substrate orientation.

Compositional analysis by AES depth profiling of a CBD-deposited SnS_x film on Mo shows the presence of a Sn-rich layer at the surface (Fig. 3a). Sulfur and some oxygen are also present, indicating that both tin sulfide and tin oxide were deposited during the SnS_x CBD process, an expected consequence of the aqueous process. Henceforth we refer to this layer as the SnS_xO_y layer. Fig. 3b shows a depth profile for a sample with two additional layers of ZnS deposited by CBD and 400 °C heat treatment, confirming the distinct Zn-rich and Sn-rich layers as seen in Fig. 2b before sulfurization. The sulfur content of the ZnS layer is higher than that of the SnS_xO_y layer, indicating that the ZnS CBD process yields a more sulfur rich film than the SnS_x process. This phenomenon is most likely due to the presence of tin hydroxide remaining from the CBD process. Since the precursor films are to be sulfurized with H_2S, this is not of concern, as the oxygen in the film is replaced with sulfur by this treatment.

The film compositions were also studied after Cu ion exchange (Fig. 4). After a 20 min soak in the ion exchange bath, there is significant incorporation of Cu into the film. The surface region is clearly comprised of a Cu-rich phase. For 2 h of ion exchange, the Cu-rich layer nearly doubled in thickness, and the Cu concentration increased deeper within the film as well. An additional 2 h of ion exchange further increased the Cu content but to a lesser degree, indicating slowing of the ion exchange process as the driving force decreases. This observed time dependence of copper incorporation was also confirmed using ICP-OES (Fig. 4d). The Cu incorporation increases significantly during the first hour, but afterwards asymptotically approaches a ratio of 0.5 for this sample set. These results demonstrate that ion exchange can be used to control the Cu content of the film.

Compositional analysis of the Cu–Zn–Sn precursor film after the 2 h sulfurization heat treatment is shown in Fig. 5a. The data indicates several important changes that have taken place in the sample. Firstly, the Cu, Sn, and Zn have interdiffused, and the composition has become remarkably uniform. Secondly, the sulfur content has dramatically increased, suggesting that the heat treatment replaced much of the oxygen with sulfur. A Zn rich stoichiometry was achieved. Although the stoichiometry is not exactly Cu_2ZnSnS_4, Zn-rich CZTS films have been shown empirically and theoretically to have superior photovoltaic performance. For instance, Katagiri et al. have empirically found that Zn-rich films achieve superior photovoltaic performance [26], and a recent theoretical study by Chen et al. concluded that Zn-rich films are beneficial for the defect properties of photovoltaic CZTS [27].

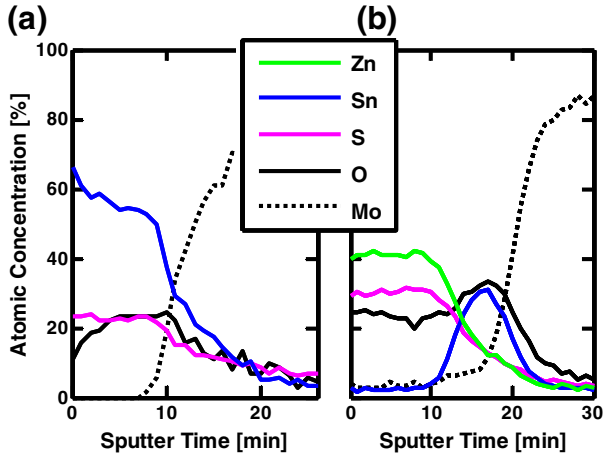

Fig. 3. AES depth profiles of CBD-deposited (a) SnS_xO_y on Mo and (b) with two additional layers of ZnS and 400 °C heat treatment.

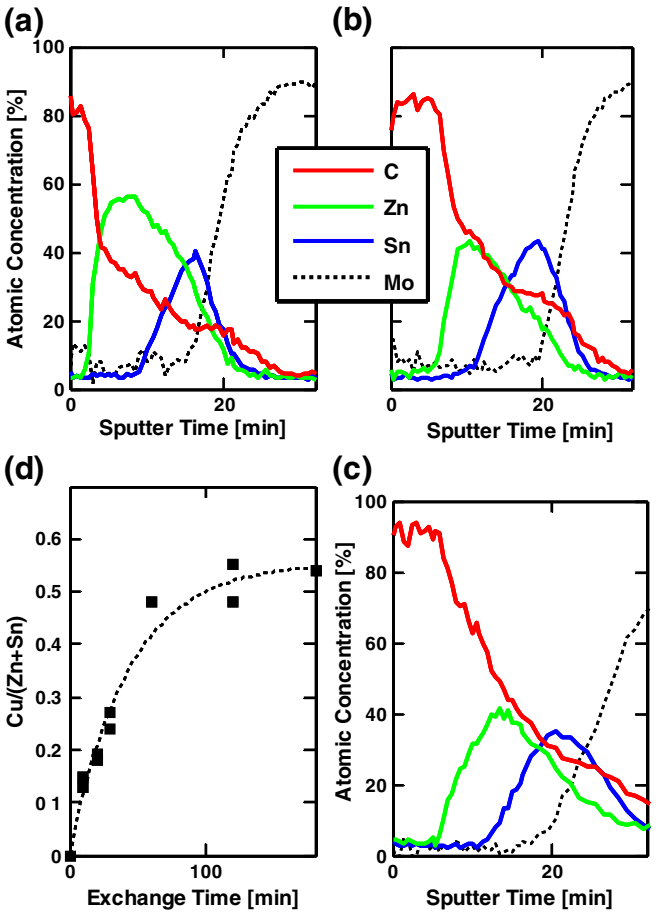

Fig. 4. AES depth profiles of Zn–Sn–S precursor film after 0.1 M Cu^{2+} ion exchange for (a) 20 min, (b) 120 min, and (c) 240 min. Shown in (d) is an ICP-OES compositional analysis as a function of time. The curve is a guide to the eye.

Katagiri et al. have used Zn-rich absorbers with a Zn-Sn ratio as high as 1.7 to improve solar cell efficiency [28]. As explained below, since the ZnS present in the film is minimal if any, we speculate that the extra Zn is in the kesterite lattice.

XRD analysis of a 2-hour sulfurized Cu–Sn–Zn precursor film on Si indicates major peaks at 28.5°, 33.0°, 47.4°, and 56.3° (Fig. 5b). These peaks are attributable to Cu_2ZnSnS_4 (112), (200), (220) and (312), respectively [29]. However, the peaks at those diffraction angles can also be attributed to β-ZnS (111), (200), (220), and (311), respectively. Both crystal phases have very similar diffraction patterns owing to their similar crystal structure – zinc blende and kesterite – and hence cannot be distinguished in this measurement. Cu_2SnS_3 also has a similar diffraction pattern. No evidence of crystalline SnS, SnS_2, or Cu_2S was observed in the diffraction pattern. Due to the overlap of many of the diffraction lines, however, XRD analysis of CZTS should be considered an estimation.

Because the XRD pattern of CZTS and β-ZnS are similar for visible peaks and the angle differences too small to distinguish within instrument accuracy, the existence of CZTS was further investigated by Raman spectroscopy, as performed previously by Fernandes et al. for sputtered samples [30]. Fig. 5c is a Raman spectrum indicating the presence of the two principal kesterite CZTS peaks at 338 cm^{-1} and 288 cm^{-1} as well as a smaller peak at 250 cm^{-1}. These peaks are well defined, suggesting that the sulfurized Cu–Sn–Zn precursor film contains the CZTS kesterite structure. Cu_2SnS_3 and other copper tin sulfides studied do not contain all three of the peaks [31]. A secondary phase of β-ZnS may be present, though the slightness of the shoulder at its principle peak (355 cm^{-1}) indicates minimal contribution of that phase if any. Furthermore, no other β-ZnS peaks are evident. A

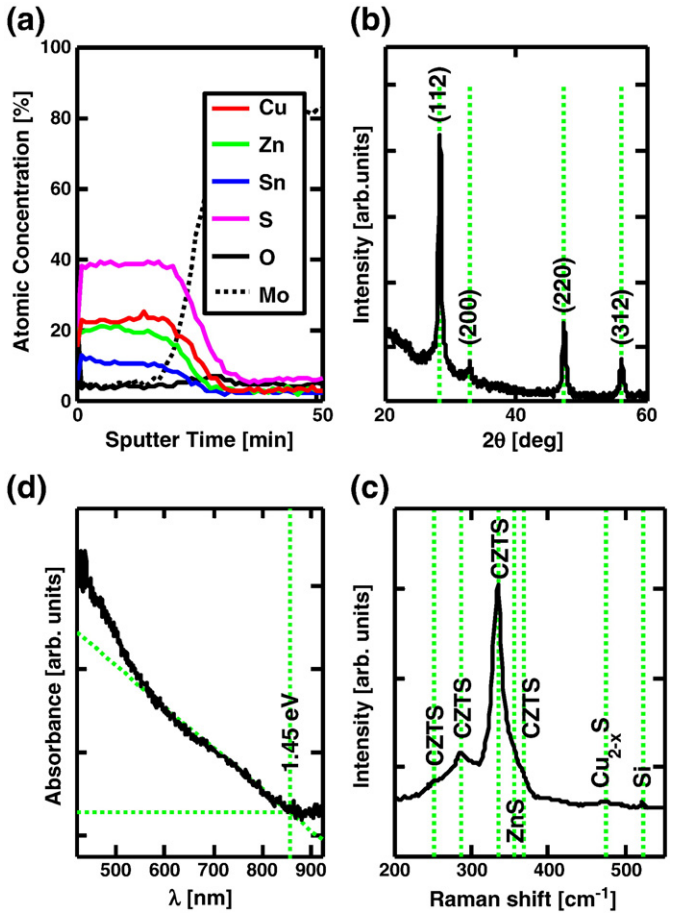

Fig. 5. 2-hour sulfurized Zn–Sn–S precursor film deposited on various substrates by CBD: (a) AES depth profile demonstrating film uniformity, (b) XRD patterns indicating kesterite crystal structure, (c) Raman spectrum with the presence of the two principle kesterite CZTS peaks, and (d) diffuse reflectance measurement of CZTS on glass indicating 1.45 eV bandgap.

very weak $Cu_{2-x}S$ peak at 475 cm^{-1} is present, which may be eliminated through KCN treatment [22].

Diffuse reflectance UV–Vis measurements (Fig. 5d) on our samples reveal a bandgap of 1.45 eV, agreeing well with other CZTS studies [32,33]. A complete solar cell device was fabricated using the process steps described above. Fig. 6 shows a cross-sectional SEM image of the final device, clearly indicating the different layers of the cell. The device was tested under AM1.5 G illumination and exhibited a photovoltaic and rectifying behavior (Fig. 7). The device achieved an

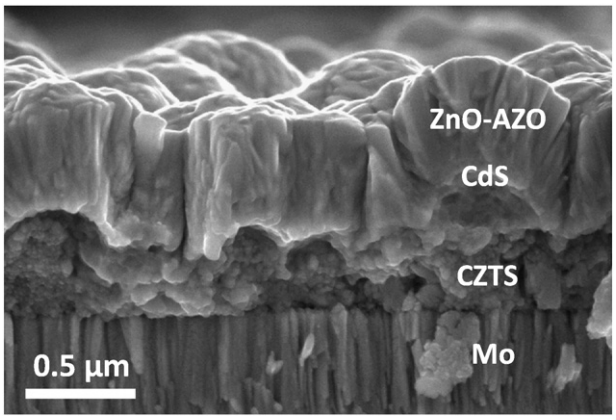

Fig. 6. SEM cross section of CZTS device.

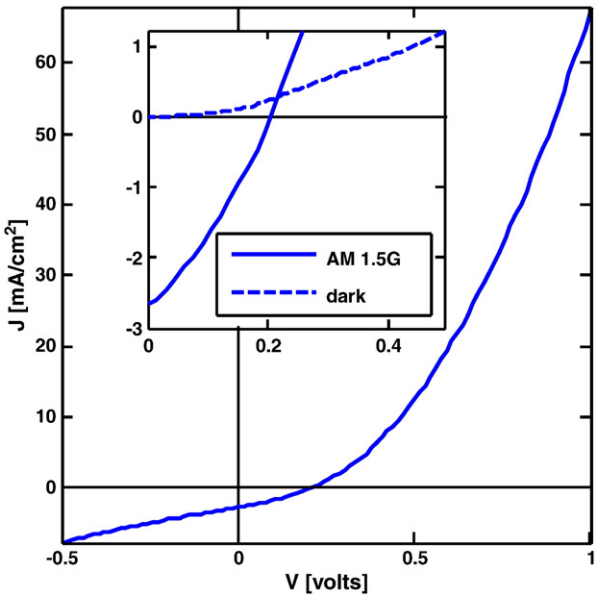

Fig. 7. Device current–voltage curve in the dark and under AM 1.5 G illumination exhibiting rectifying and photovoltaic behavior.

open circuit voltage of 210 mV, a short circuit current of 2.4 mA/cm^2, and an energy conversion efficiency of 0.16%. Factors contributing to the low device performance most likely include small grain size and non-optimized thicknesses for each of the device layers. When compared to the dark current in the inset of Fig. 7, the principle of superposition does not appear to apply to the device under illumination, indicating that the photogenerated current varies with voltage, which may be a sign of defective polycrystalline material.

4. Conclusion

This work demonstrates that CZTS thin-film photovoltaic absorber layers can be deposited through an aqueous process. The four elements of interest were incorporated through chemical bath deposition and ion exchange into a precursor stack, which was transformed into CZTS by sulfurization. While more detailed work on the correlation between deposition/soak times and final stoichiometry is in progress, the main process steps are outlined here. The method is not only conducive to large area production but also avoids the use of expensive and complicated equipment. Although the initial device performance was modest due to small grain size and insufficient absorber thickness, we believe that most of these issues can be addressed with further research. Our most recent chalcogenide thin films by CBD are thicker and exhibit larger grains. Given that Cd-free, thin-film buffer layers can be deposited by CBD [34] and that new transparent conductors deposited by solution have been reported [35,36], the method presented here can be integrated into a largely solution process for an inorganic photovoltaic device of earth-abundant and non-toxic materials. The chemical bath technique can also be tailored to produce materials of various optical and electronic properties. For instance, a similar process could be designed for $Cu_2ZnSn(Se,S)_4$, since CBD of ZnSe and CuSe has been established [19].

Acknowledgements

We thank Justin Opatkiewicz for help with Raman spectroscopy and Dan Chawla for assistance with XRD and device preparation. The Global Climate and Energy Project is gratefully acknowledged for the initial funding of this research. Studies were carried out as part of the Center on Nanostructuring for Efficient Energy Conversion, an EFRC funded by the U.S. Department of Energy, Office of Basic Energy

Sciences under Award Number DE-SC0001060. AW received support under the National Science Foundation Grant CBET 0930098.

References

[1] A. Feltrin, A. Freundlich, Renew. Energy 33 (2008) 180.
[2] H. Katagiri, K. Jimbo, W.S. Maw, K. Oishi, M. Yamazaki, H. Araki, A. Takeuchi, Thin Solid Films 517 (2009) 2455.
[3] N. Nakayama, K. Ito, Appl. Surf. Sci. 92 (1996) 171.
[4] H. Katagiri, N. Sasaguchi, S. Hando, S. Hoshino, J. Ohashi, T. Yokota, Sol. Energy Mater. Sol. Cells 49 (1997) 407.
[5] J.S. Seol, S.Y. Lee, J.C. Lee, H.D. Nam, K.H. Kim, Sol. Energy Mater. Sol. Cells 75 (2003) 155.
[6] K. Tanaka, N. Moritake, H. Uchiki, Sol. Energy Mater. Sol. Cells 91 (2007) 1199.
[7] H. Katagiri, K. Jimbo, S. Yamada, T. Kamimura, W.S. Maw, T. Fukano, T. Ito, T. Motohiro, Appl. Phys. Express 1 (2008) 041201.
[8] J.J. Scragg, P.J. Dale, L.M. Peter, G. Zoppi, I. Forbes, Phys. Status Solidi 245 (2008) 1772.
[9] C. Steinhagen, M.G. Panthani, V. Akhavan, B. Goodfellow, B. Koo, B.A. Korgel, J. Am. Chem. Soc. 131 (2009) 12554.
[10] Q. Guo, H.W. Hillhouse, R. Agrawalet, J. Am. Chem. Soc. 131 (2009) 11673.
[11] S.C. Riha, B.A. Parkinson, A.L. Prieto, J. Am. Chem. Soc. 131 (2009) 12054.
[12] T.K. Todorov, K.B. Reuter, D.B. Mitzi, Adv. Mater. 22 (2010) E156.
[13] R.S. Mane, C.D. Lokhande, Mater. Chem. Phys. 65 (2000) 1.
[14] R.D. Engelken, S. Alia, L.N. Changa, C. Brinkleya, K. Turnera, C. Hester, Mater. Lett. 10 (1990) 264.
[15] P.K. Nair, V.M. Garcia, O. Gomez-Daza, M.T.S. Nair, Semicond. Sci. Technol. 16 (2001) 855.
[16] M.T.S. Nair, P.K. Nair, Semicond. Sci. Technol. 6 (1991) 132L.
[17] A. Cheng, D.B. Fan, H. Wang, B.W. Liu, Y.C. Zhang, H. Yan, Semicond. Sci. Technol. 18 (2003) 676.
[18] D.H. Son, S.M. Hughes, Y.D. Yin, A.P. Alivisatos, Science 306 (2004) 1009.
[19] C.A. Estrada, R.A. Zingaro, E.A. Meyers, P.K. Nair, M.T.S. Nair, Thin Solid Films 247 (1994) 208.
[20] L. Dloczik, R. Koenenkamp, J. Solid State Electrochem. 8 (2004) 142.
[21] J.R. Bakke, J.S. King, H.J. Jung, R. Sinclair, S.F. Bent, Thin Solid Films 518 (2010) 5400.
[22] P.A. Fernandes, P.M.P. Salomé, A.F. da Cunha, Semicond. Sci. Technol. 24 (2009) 105013.
[23] K. Ramanathan, M.A. Contreras, C.L. Perkins, S. Asher, F.S. Hasoon, J. Keane, D. Young, M. Romero, W. Metzger, R. Noufi, J. Ward, A. Duda, Prog. Photovolt. Res. Appl. 11 (2003) 225.
[24] C.D. Lokhande, Mater. Chem. Phys. 27 (1991) 1.
[25] D. Olekseyuk, I.V. Dudchak, L.V. Piskach, J. Alloys Compd. 368 (2004) 135.
[26] H. Katagiri, K. Jimbo, M. Tahara, H. Araki, K. Oishi, Thin-film compound semiconductor photovoltaics, Warrendale, U.S.A., april 13-17, 2009, in: A. Yamada, C. Heske, M. Contreras, M. Igalson, S.J.C. Irvine (Eds.), Materials Research Society Symposium Proceedings, 1165, 2009, p. M04-01.
[27] S. Chen, X.G. Gong, A. Walsh, S.-H. Wei, Appl. Phys. Lett. 96 (2010) 021902.
[28] H. Katagiri, K. Jimbo, W.S. Maw, K. Oishi, M. Yamazaki, H. Araki, A. Takeuchi, Thin Solid Films 517 (2009) 2455.
[29] Powder Diffraction File, International Centre for Diffraction Data, PDF 26–0575 (Cu2ZnSnS4), PDF 01–071–5976 (cubic ZnS), PDF 01–089–4714 (tetragonal Cu2SnS3) (accessed 10 Sept 2009).
[30] P.A. Fernandes, P.M.P. Salomé, A.F. da Cunha, Thin Solid Films 517 (2009) 2519.
[31] P.A. Fernandes, P.M.P. Salomé, A.F. da Cunha, J. Phys. D Appl. Phys. 43 (2010) 215403.
[32] J.J. Scragg, P.J. Dale, L.M. Peter, Electrochem. Commun. 10 (2008) 639.
[33] K. Moriya, T. Kunihiko, H. Uchiki, Jpn. J. Appl. Phys. 47 (2008) 602.
[34] T. Nakada, M. Mizutani, Jpn. J. Appl. Phys. 41 (2002) 165.
[35] J.Y. Lee, S.T. Connor, Y. Cui, P. Peumans, Nano Lett. 8 (2008) 689.
[36] H. Ago, K. Petritsch, M.S.P. Shaffer, A.H. Windle, R.H. Friend, Adv. Mater. 11 (1999) 1281.